Available online at www.sciencedirect.com

ScienceDirect

Procedia Manufacturing 14 (2017) 17–29

Procedia MANUFACTURING

www.elsevier.com/locate/procedia

17th Machining Innovations Conference for Aerospace Industry, MIC 2017, 6-7 December 2017, Garbsen, Germany

Machining of large scaled CFRP-Parts with mobile CNC-based robotic system in aerospace industry

Dipl.-Ing. Christian Möller[a]*; Hans Christian Schmidt[a], M.Sc.; Philip Koch[a], M.Sc.; Christian Böhlmann[a], M.Eng.; Dipl.-Ing. Simon-Markus Kothe[a]; PD Dr.-Ing. habil. Jörg Wollnack[b]; Prof. Dr.-Ing. Wolfgang Hintze[b]

[a]*Fraunhofer IFAM, Ottenbecker Damm 12, 21684 Stade, Germany*
[b]*Technische Universität Hamburg, 21071 Hamburg, Germany*

Abstract

Industrial robots have already demonstrated their advantages in smart and efficient production in a wide field of applications and industries. However, their use for machining of structural aircraft components is still impeded by the disadvantage of low absolute accuracy, sensitivity to process loads and limited workspace compared to large machining centers.
A mobile robotic system is presented as a new approach for machining applications of large aircraft components. The system presented in this paper consists of a CNC-based serial robot kinematic with additional secondary encoder systems on every axis. The entire system is based on a *Siemens* CNC control, which evolves the robot to a full-featured machine tool. This setup enables additional possibilities for the implementation of extended control strategies and advanced calibration routines. Thus, high demands and challenging tolerances in aircraft manufacturing will be fulfilled, so that process times and investment cost can be reduced significantly.

Peer-review under responsibility of the scientific committee of the 17th Machining Innovations Conference for Aerospace Industry.

Keywords: robotics; automation; CNC machining; secondary encoders; robot calibration

* Corresponding author. Tel.: +49-4141-78707-261; fax: +49-4141-78707-682.
E-mail address: christian.moeller@ifam.fraunhofer.de

2351-9789
Peer-review under responsibility of the scientific committee of the 17th Machining Innovations Conference for Aerospace Industry.
10.1016/j.promfg.2017.11.003

1. Introduction

Within the scope of steady growth of word wide air traffic, which will double in the next 15 years, the aerospace industry launches multiple approaches of automating production processes [1]. The current production rate led to an order backlog of approx. 12,500 aircrafts for Boeing and Airbus [2,3] leading to withdrawal periods of over 8 years, when production rates remain constant. The goal of the aerospace industry tends away from static special machining centers towards universally useable plant concepts. Machining of large carbon fibre reinforced polymers (CFRP) structures is nowadays performed by large and heavy special portal machines. The application of industrial robots is mostly limited to processes that are repeatable so that processes and robot paths can be taught.

To build up alternative and further applications for industrial robots e.g. the milling of CFRP parts, certain current limits must be observed and overcome. The absolute accuracy and stiffness of industrial robots are affected by multiple environmental conditions. Changes in ambient temperature lead to thermal expansion and deviations of the end-effector position in millimeter range [4] and process forces and even the weight of robot links themselves create torques that induce errors due to limited tilting rigidity of gears and bearings [5].

This paper will show approaches on how these disadvantages can be overcome or at least decreased. Because of the variety of possible improvements this work will focus mainly on the integration of additional secondary encoder systems in the robot joints to reduce effects of gear backlash and resilience. It is examined on how secondary encoders help improving accuracy and "virtual" stiffness of the robotic system as well as the robot path accuracy during motion. For further improvements including additional machining and compensation strategies or measurement and sensor devices, attention is invited to [6–8].

2. State of the art in machining of large CFRP structures

Currently milling operations of large CFRP structures are primarily executed by conventional machining systems in portal design that cause very high investment costs due to the large dimensions of the workpieces and special heavy foundations to carry the machine weight. This machining concept is comparatively unproductive, because of the missing possibility of parallel machining operations that would speed up the building process immensely [5,9].

Machining with industrial robots is still mostly represented in automotive industry, where milling of plastic components with high rates are common. Process forces and changes in process forces are very low, which favors the kinematic and structural behavior of the robot compared to metal or CFRP-milling processes [10]. Additionally changes of the workpiece shape rarely apply [11]. That way fairly constant process scope conditions can be presumed. In this case the milling path is taught and iteratively optimized until the demands are reached. Keeping the thermal conditions of the shop floor constant and by providing rigid holding fixtures the achieved machining accuracy is in range of the robots repeatability, which makes the process very reproducible.

These strategies cannot be applied in aerospace manufacturing, especially in CFRP machining. Due to uniqueness and variety of every workpiece and concurrently high tolerance demands, every part needs an adaptive process, if robot machining should be utilized. Compared to machining centers, especially low stiffness and absolute accuracy of industrial robots due to the serial kinematic structure as well as small working volume represent a challenge. That is why robot workspace, accuracy and stiffness need improvements, which is shown by the approach in this present work.

3. Mobile robotic machining system

To extend the workspace of robotic systems, two approaches are common. For one dimensional movements many times linear axis are used, which is suitable for large and plane workpieces and a static shop floor. However the need for more flexible arrangements demands multidimensional movements of the machining system. Therefore mobile platforms can be utilized. The engineering process of these platforms aims for high stiffness and rigidity as if the robot would be mounted on a machine interface. At the same time the whole system needs to be flexible and should satisfy all demands regarding large and complex workspaces.

Figure 1. Mobile Robotic System for machining applications

The system used during this work is shown in Figure 1. It consists of a self-built triangular shaped platform including all desired periphery for the milling process such as drives, dust-removal systems and spindle cooling devices. During machining the platform is set on three defined footprints to prevent tilting and to cancel out the resilience of the drives. For movements the platform extends wheels that are able to move in any direction and allow linear movements and rotating around the vertical axis.

The platform is equipped with a machining robot based on the *Max 150* by *MABI Robotic* that uses *Siemens* drives and a standard *SINUMERIK 840D sl* to ensure maximum compatibility and comparability to machining centers. The robot reaches up to 2.2 meters, can carry 150 kg at the end-effector and is equipped with a 19 kW high speed spindle *SLQ120* at the flange. A process monitoring device by *Artis* – integrated in the tool holder – measures machining forces. The mass of the entire system is about 5,500 kg.

3.1. CNC machining robot with Sinumerik 840D sl

Using a standard CNC control establishes the possibility to use the robot without further knowledge about robotic controls. That way users who are experienced in operating standard machining centers used in aerospace industry do not need additional training or instructions. However, the main reason for using a standard *Siemens* control is the possibility of utilizing various software modules that allow custom adjustments for machining operations, such as strategies for milling of freeform surfaces and software interfaces that allow manipulation of the milling path during operation. The possibility to add custom compile cycles is necessary to include additional measurement devices in the control strategy such as secondary encoders that will be mentioned later on. The advanced user gets access to the so called “Universal Compensation Interface” (UCI) that mainly provides the possibility to adjust the robot trajectory online. Within the UCI the existence of the UCI-App enables the user to read and write parameters of the control as well as providing an interface to include custom C++-code and algorithms that are used to configure advanced control strategies.

4. Secondary encoder measurement system

The application of additional measurement systems like secondary encoders in industrial robots for machining is acknowledged in different examinations [12] and is slowly applied in serial products of robot manufacturers like FANUC [13]. The benefit of additional secondary encoders on the output side of every joint is direct knowledge about deformation and deviation effects that occur in the powertrain of the axis.

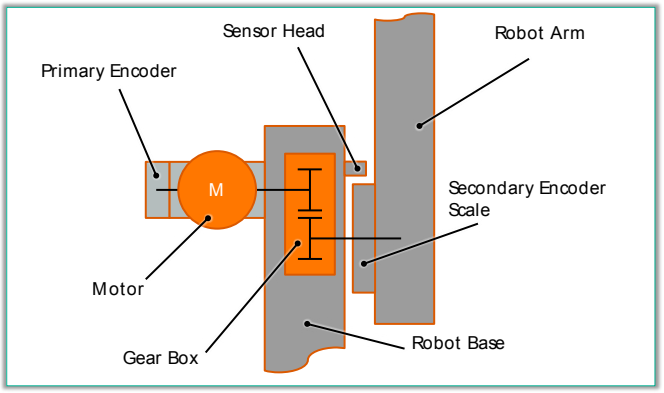

Figure 2. Schematic illustration of robot axis powertrain

The powertrain consists of the gear box and bearings that deform under the impact of external torques due to tare weight or process forces. This resilience prevents recognition of tool center point (TCP) deviations by the primary encoders on the motor side. Especially during direction changes reversal effects like gear backlash remain unrecognized without secondary encoders. Thereby new levels of accuracy and repeatability can be reached, especially during machining tasks, where TCP deflection can be reduced significantly [14]. The tests results later on in this work prove these statements.

4.1. Implementation

All principles have the setup in common. Coded rings or tapes are applied to one link while a sensor head is mounted on the adjacent link to detect the differential motion. Basically three different measuring principles for secondary encoders are common: Magnetic, inductive and optical measurements. Magnetic tapes are cheaper and easy to apply even on completed robotic systems. However the measurement resolution is comparably low. Because of the gear ratio lying typically axis depending between 150 and 250, the resolution of secondary encoders needs to be significantly higher than the primary encoders to be comparable. Optical measurement techniques offer very high resolutions and are often times the number one choice, if the result only needs to be precise. On the other hand optical systems are susceptible to dust and rather expensive – especially if every axis should be equipped.

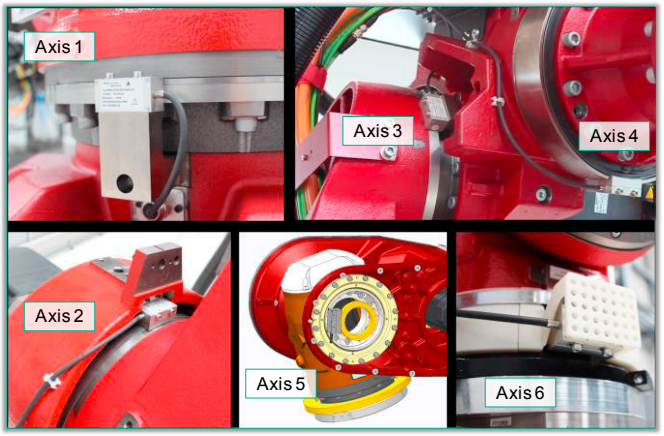

Figure 3. Implementation of secondary encoders in *MABI Max 150*

That is why an inductive solution was chosen. The overall resolution is sufficient, especially for the most important first three axes, and it offers a robust measurement principle. In case of the inductive measuring principle the measuring scale is a stainless steel tape onto that a high precise periodical graduation has been etched. The sensor head consists of a coil structure aligned in the direction of measurement, which generates two sinusoidal signals with

90° phase shift that can be evaluated by the following integrated circuits [15]. An additional reference track extends the incremental measurement to an absolute measurement.

4.2. Measurement accuracy

Although rings are used, the basic measurement is linear and will only be transformed in the robot control. That is why the effective angle resolution is dependent on the axis radius and therefore different for each axis. The incremental resolution of the utilized *Amo AMOSIN® Absolute angle measurement system* is 0.25 µm [15]. That leads to following angle resolutions per axis.

Table 1. Axis data for *MABI Max 150*

	Axis 1	Axis 2	Axis 3	Axis 4	Axis 5	Axis 6
diameter [mm]	459.0	327.6	287.1	287.1	164.6	229.8
resolution [arcsec]	0.22	0.31	0.35	0.35	0.62	0.44

It should be noted, that the effective axis angel resolutions are still lower than the primary encoder resolution after consideration of gear ratio. However, they are sufficient for the further use in the control strategies described below.

5. Control strategies: MMS and DMS+

Current robot controls mainly use cascaded controls that are shown in Figure 4. Each axis is described as a single-input single-output system with internal current control cascade, speed control cascade and outer position control cascade. Most systems additionally use pre-controls for torque and speed to optimize the dynamic behavior of the control loop [16]. The internal cascades work with shorter cycle times than the position control loop, whose cycle-time is 0.5 milliseconds in the present case. Here this setup is named “motor measurement system” (MMS).

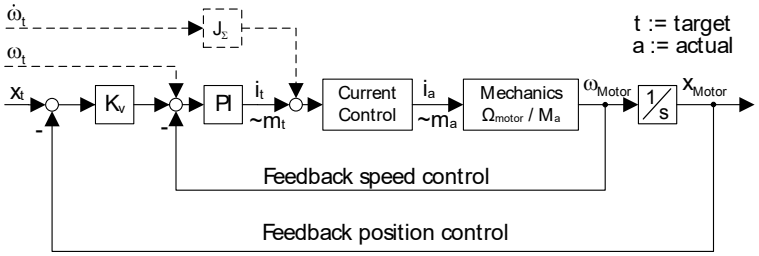

Figure 4. Standard robot cascade control

The parameters of each individual control are configured conservatively in a way that the robotic system remains stable in its entire workspace and that cross-coupling effects can be neglected [17]. With the addition of secondary encoders, the primary encoders are still necessary for all following control strategies to measure (angular) speed and position values for the inner cascades.

FANUC was the one of the first robot manufacturers to implement secondary encoders in industrial robots in serial production and in the control law. The cascade has been modified by adding an additional cascade that feeds back the directly measured joint position to the position input of the standard cascade [18]. Because of the working principle of cascade controls, this additional outer cascades cycle time can at most be in range of the position control loops cycle time, which lets the system only react to slow or static disturbances.

To exploit the full potential of the secondary encoders the *Siemens* “Advanced Position Control” (APC) is used to get access to the inner cascades [19]. APC is divided into two parts. Figure 5 shows these in green and orange.

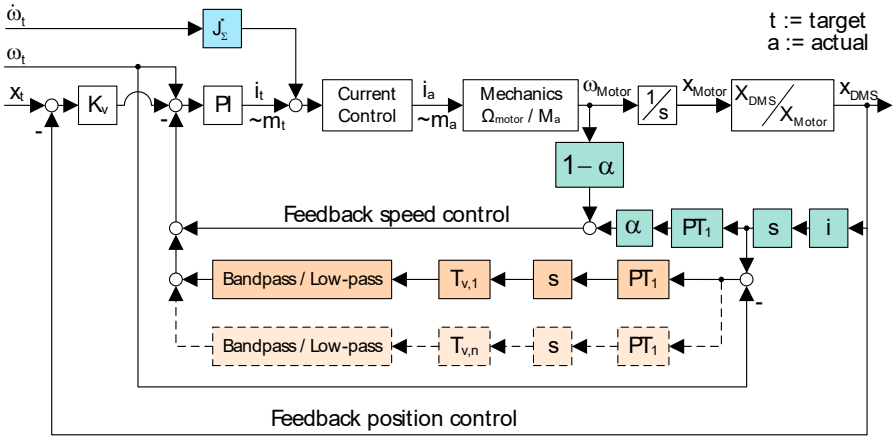

Figure 5. Advanced control strategy with individual mode damping

The secondary encoder position values are named x_{DMS} for “Direct Measurement System” (DMS). The actual additional control is pictured by the green branch. Parameter α allows an individual compilation of primary and secondary encoder values. E.g. for $\alpha = 0$ the control law is identical with MMS and the standard robot cascade control. It is worth mentioning that the feedback of the secondary encoder directly attaches to the speed control cascade. That way it is possible to react even to fast external disturbances and to use the secondary encoders in situations of high acceleration and velocity.

The orange branch is used to damp specific modes of the closed loop control with bandpass/low-pass filters. This can be executed several times and for every mode separately. Because of the usage of secondary encoders, no models for weight compensations are necessary. The only addition is the implementation of an adaptive torque pre-control that is described in the following section.

6. Calibration and compensation strategies

6.1. Calibration

A precondition for high path accuracy is high absolute accuracy in the stationary case. To move the end effector to a certain position and orientation, the corresponding joint angles have to be calculated first. After that the servomotors are commanded to move to the calculated angles, taking into account the transmission ratio of the gearings. The process of calculating the joint angles from the given pose is called “inverse kinematics”. For this process a kinematic model of the robot is used. Deviations of the kinematic model from the real kinematic lead to errors in the calculated joint angles and consequently to wrong end effector positions. Thus, to reach a high absolute positioning accuracy, a precise kinematic model is required. For the application and results in this work the parameters of the kinematic model cannot simply be taken from the production documents because manufacturing tolerances would lead to positioning errors of several millimeters at the milling tool. Therefore, the values of the parameters are obtained by means of a calibration process. Additionally an extended kinematic model is used, which represents the real kinematic more precisely than the model provided by the manufacturer of the CNC control. For the kinematic model a combination of the Denavit-Hartenberg method with the Hayati-Mirmirani method is used [20]. Additionally the eccentricities of the scale tapes of the secondary encoders are covered by the kinematic model.

For calibration the robot is moved to about 100 different poses distributed in the global workspace. Each of the poses is measured at the end effector by a *Leica AT401 Laser Tracker*. Instead of a milling tool, a calibration tool is inserted into the spindle. The calibration tool is equipped with three retro reflectors; the position of these reflectors can be measured by the Laser Tracker. The reflector positions define the “measurement frame”. With the kinematic model the position of the measurement frame relative to the Laser Tracker can be calculated. The goal of the calibration algorithm is to find a set of parameters for the kinematic model so that the deviations between the calculated

positions of the measurement frame and the measured positions of the measurement frame become as small as possible. In other words, the sum of squared deviations is minimized [14]:

$$\min_{\boldsymbol{p}} \left\{ \sum_{i=1}^{n} \|\boldsymbol{r}_i(\boldsymbol{p})\|_2^2 \right\} \rightarrow \boldsymbol{p}_{\text{opt}} \tag{1}$$

$$\boldsymbol{r}_i = \boldsymbol{f}_{RPY} \left(\left({}^{LT}\boldsymbol{T}_{M,mod}(\boldsymbol{p}, \boldsymbol{x}_i) \right)^{-1} {}^{LT}\boldsymbol{T}_{M,meas}(\boldsymbol{p}, \boldsymbol{x}_i) \right) \tag{2}$$

where:

$\mathbf{p}$:	parameter vector of the kinematic model
n:	number of measured poses (here about 100)
$\mathbf{r}_i$:	residual for pose i
$\mathbf{p}_{\text{opt}}$:	vector of optimized parameters
$\mathbf{f}_{\text{RPY}}$:	function which converts a homogenious transformation matrix into a roll-pitch-yaw pose vector
${}^{\text{LT}}\mathbf{T}_{\text{M,meas}}$:	homogenious matrix which transforms a vector from the measurement frame to the laser tracker frame; index “mod”: calculated with kinematic model; index “meas”: measured with Laser Tracker

The minimization algorithm that is utilized here chooses the sequence in which the parameters are optimized depending on the sensitivity of the parameters. The sensitivity is a measure for the influence of measurement errors on the optimized parameters. Additionally, the optimization is performed hierarchically: First the parameters with the heaviest impact on the accuracy are optimized. Then, in the following iterations, less important parameters are optimized. With the resulting kinematic model the joint angles can be calculated if the positional relationship between the measurement frame and the robot base frame is given.

To use the kinematic model for a milling process, the positional relationship between the milling tool and the measurement frame must be known. This relationship is measured with help of a tool presetter. The spindle accommodates the milling tools or the calibration tool via hollow shank tapers (HSK). The tool presetter is used twice: First the positional relationship between the measurement frame and the HSK is measured; second the length between the HSK and the milling tool tip is measured.

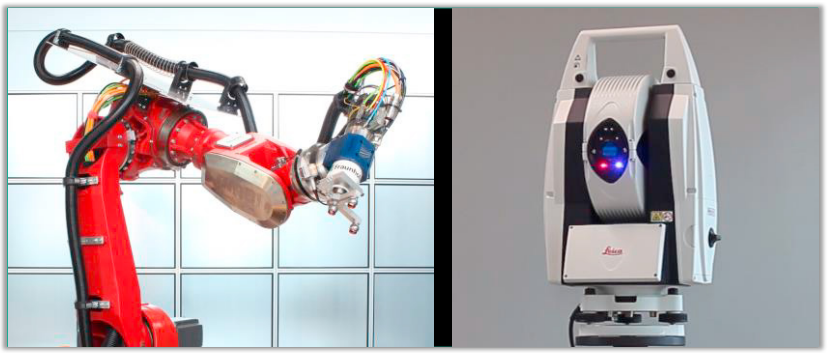

Figure 6. Robot with calibration device and Laser Tracker AT401

The extended kinematic model is applied via a custom UCI-App developed at the *Fraunhofer IFAM*. The App calculates the inverse kinematics iteratively and therefore can take all modeled effects into account. The hard-real-time capability of the implemented algorithms enables the App to calculate the inverse kinematics in each IPO-cycle. Therefore the calculations do not need to be performed offline and after the calibration is completed, no extra hardware is needed to increase the accuracy of the robot. Additionally, the solution is safe because the trajectories (joint angles over time), calculated by the manufacturer’s algorithms, are just modified and not replaced.

6.2. Friction compensation

Disturbances due to friction effects within the gears and bearings can lead to considerable path errors. When the direction of movement changes, the velocity passes zero. Therefore the friction changes from sliding friction to static friction and again back to sliding friction. This leads to abrupt changes of the friction forces and cannot appropriately be handled by the cascade controllers alone.

The Siemens CNC control provides the option of friction compensation. This is achieved by a velocity pre-control signal that has the shape of a step signal that fades away quickly. The size of the step depends on the current movement of the robot.

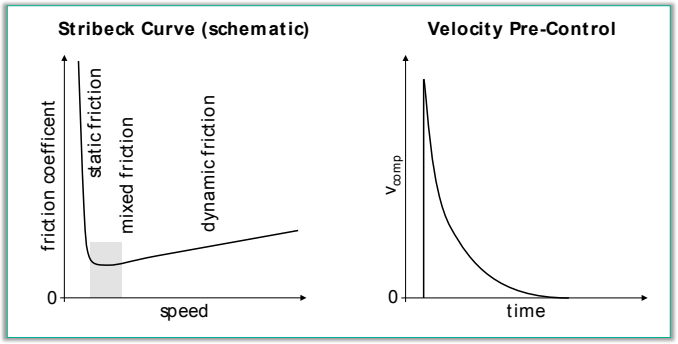

Figure 7. Stribeck curve [21] and friction pre-control signal

6.3. Torque pre-control

For machine tools a common approach to obtain higher path accuracies is the use of torque pre-control. With this technique disturbances due to mass inertias can be compensated. Based on the reference acceleration and the effective moment of inertia the required torque of an axis can be estimated and therefore taken into account by the controller before the mass inertias lead to disturbances of the contollers. Usually, for machine tools with cartesian structure, it is a very good approximation to assume that the effective moments of inertias are constant.

This does not hold for industrial robot arms with serial structure. The effective moments of inertia heavily depend on the current position of the robot. Siemens solved that problem with a plug-in called “ROCO”. The plug-in calculates the effective moments of inertia adaptively using a mathematical model of the robot which considers the mass and the inertia tensor of each link.

7. Validation and test results

As already mentioned the accuracy is an important parameter for milling applications. Another essential aspect is the repeatability of the robot. In the following chapter, three different validation tests will be presented to evaluate the potential of the secondary encoders by means of the described control strategies. On the contrary to the method described in ISO 9283, a repeatability test with different approach directions is performed. Moreover stiffness tests are executed on the robot and ballbar tests for standard milling machines are performed during the development process.

7.1. Bi-directional repeatability

For many applications, especially pick and place applications, the repeatability of a robot as defined in [22] is an important parameter. It describes how precise the target position is reached when repeatedly approached from the same direction. For a milling robot this parameter is also an important characteristic, except in this case the robot has to approach the target position from random directions.

In this work, several target locations distributed in robot´s work volume are tested from two different directions for repeatability as suggested in [23]. The TCP of the robot moves to the given target position thirty times from alternating

directions. The actual reached position is measured by a *Leica Laser Tracker AT960* and pictured in two point clouds depending on the approach direction [24]. Two pre-poses are defined in a way that the robot has to move every joint to reach to the given target joint angles:

$$\boldsymbol{p}_{pre\uparrow} = \boldsymbol{p}_{set} - \begin{pmatrix} \delta \\ \delta \\ \delta \\ \delta \\ \delta \\ \delta \end{pmatrix} \quad and \quad \boldsymbol{p}_{pre\downarrow} = \boldsymbol{p}_{set} + \begin{pmatrix} \delta \\ \delta \\ \delta \\ \delta \\ \delta \\ \delta \end{pmatrix} \tag{3}$$

where:

$\mathbf{p}_{\mathrm{set}}$: target position,
$\mathbf{p}_{\mathrm{pre}\uparrow}$: Pre-pose for positive approach direction,
$\mathbf{p}_{\mathrm{pre}\downarrow}$: Pre-pose for negative approach direction,
δ : angle (here $\delta = 2°$)

The equations also describe the two approach directions. The TCP of the robot starts moving from the pre-poses $\mathbf{p}_{\mathrm{pre}\uparrow}$ and $\mathbf{p}_{\mathrm{pre}\downarrow}$ to the target position $\mathbf{p}_{\mathrm{set}}$. According to [25] the centers $\mathbf{x}_{\uparrow}$ and $\mathbf{x}_{\downarrow}$ of the two point clouds have to be calculated. The distance u between the two centers is called reversal range and is shown in Figure 8 (a). Additionally the distribution of the single values of the measured positions around the centers $\mathbf{x}_{\uparrow}$ and $\mathbf{x}_{\downarrow}$ is illustrated.

The bi-directional repeatability P_U can be calculated by means of the standard deviations $s_{\uparrow}$ (distances between center $\mathbf{x}_{\uparrow}$ and measured data of the target position reached from $\mathbf{p}_{\mathrm{pre}\uparrow}$) and $s_{\downarrow}$ (distances between center $\mathbf{x}_{\downarrow}$ and measured data of the target position reached from $\mathbf{p}_{\mathrm{pre}\downarrow}$) as well as u

$$P_U = u + 3(s_{\uparrow} + s_{\downarrow}). \tag{4}$$

The described test is performed on several positions with and without corrections from secondary encoder feedback. The results of one of the target positions are presented in Figure 8 (b). Bi-directional repeatability test of the robot with only internal encoders is shown on the left, whereas on the right, the robot with feedback of secondary encoders is used.

By using the secondary encoders the reversal range is reduced from 0.23 mm to 0.03 mm. Also the bi-directional repeatability is reduced significantly (0.29 mm to 0.08 mm) because the mean standard deviation remains similar and is very small compared to the reversal range.

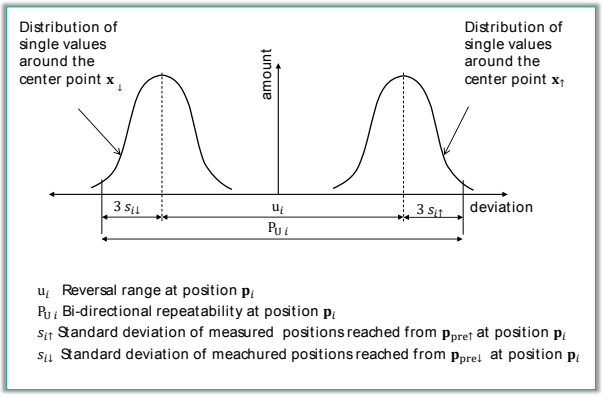

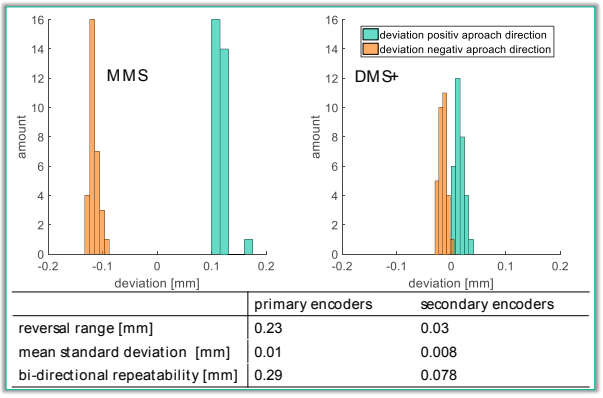

	primary encoders	secondary encoders
reversal range [mm]	0.23	0.03
mean standard deviation [mm]	0.01	0.008
bi-directional repeatability [mm]	0.29	0.078

Figure 8. Specification of bi-directional repeatability (a) and results of positioning test (b)

7.2. Stiffness test

Forces that occur during the milling process can lead to strong TCP deflection. This effect has already been discussed in several publications as mentioned before [5], [11]. With feedback of secondary encoders on robot joints, the deformation and backlash of gears caused by milling forces can be detected and compensated. The performed test shows the behavior of robot systems with use of secondary encoders compared to a robot system with conventional control strategies.

The displacement of the TCP caused by forces is shown in Figure 9 (a). In addition to a reduced reverse effect h which could already be seen in the previous test, the maximum displacement v_{max} can be reduced by use of secondary encoders significantly. The results of the performed stiffness test are shown in Figure 9 (b). An applied force is incremented and decremented stepwise and the displacement of the TCP is measured. The force is applied at the TCP in x- and in y- direction.

During the test the TCP of the robot was situated in a typical machining position (approx. 1.7 meters away from the robot base) and the drive control is kept active. In both, the x- and the y- direction of applied load, the maximal displacement was reduced. In y-direction the improvement is particularly better. The differences between both directions lead back to the different flow of forces. For example, for a y-direction large torque applies on the gear of the first axis due to large lever effects.

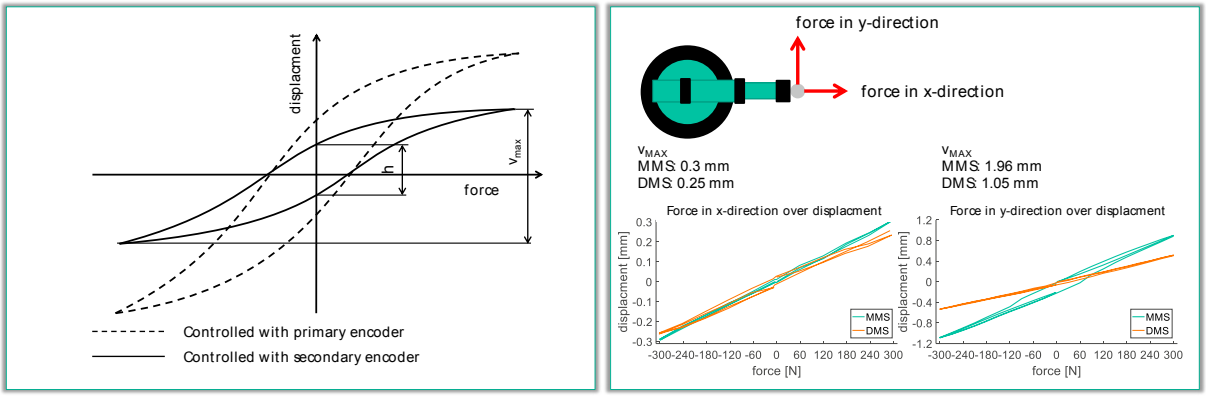

Figure 9. Schematic curve of displacement over force (a) and results of stiffness test (b)

7.3. Ballbar test

The ballbar test allows checking geometric parameters and dynamic behavior of a machining center in an easy way and is defined in [26]. Nevertheless, several circular tests with the ballbar system *QC20-W* from *Renishaw* are performed with the robot at different stages of the development process to achieve robot optimization.

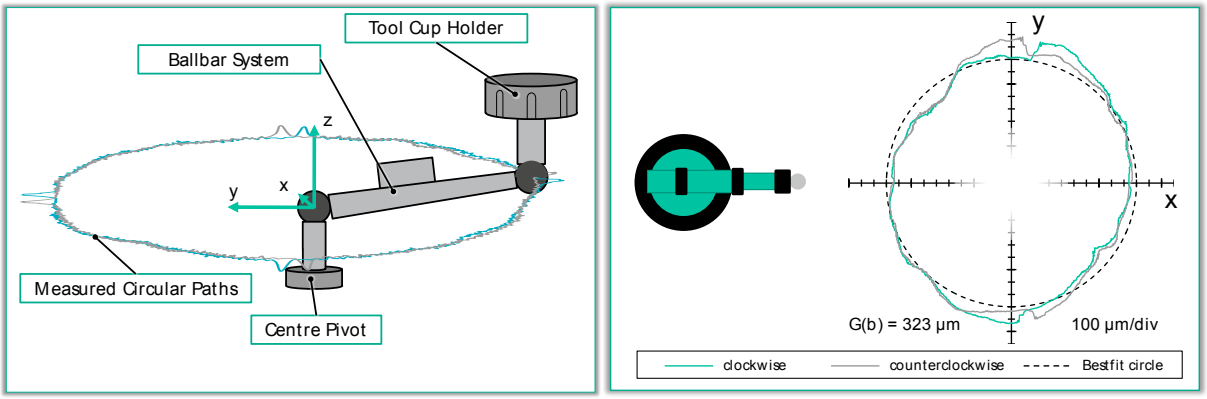

Figure 10. Setup to perform circular tests (a) and results of circular test after first commissioning (b)

A sketch of the measurement system is shown in Figure 10 (a). On the machine bench, a center pivot is mounted while the tool cup holder is attached to the machining spindle. The measurement system is held between these parts by magnets. The TCP moves clockwise and counterclockwise around the center and the ballbar measures changes in distance of the spindle to the center of the measurement system. To fulfill a circular movement, a robot usually has to move all six axes instead of only two which is the case for conventional machining centers. Thus, it is in some cases difficult to correlate the occurring positioning error of the robot TCP to their exact cause during circular test.

After each state of development, circular tests are performed under consistent conditions (radius r = 150 mm, feed rate v = 1000 mm/min). The bi-directional circular deviation G(b) is calculated according to [26] and considered as comparative parameter for improvement of robots optimization. To identify this parameter, two concentric circles enveloping the two measured paths are calculated. The difference of radiuses of these two circles descries the bi-directional circular deviation.

The circular test result after the commissioning of the robot (without secondary encoder feedback) is presented in Figure 10 (b). For this setup the bi-directional circular deviation is 323 µm.

Further development steps are shown in Figure 11 (a). On the left, the result of circular test with feedback from secondary encoders is shown. The bi-directional circular deviation is raised to 385 µm. Nevertheless the clockwise and counterclockwise paths match with each other in a more accurate way suggesting a reduction of reversal effects. In addition to this, it is also observed that where the joints have to pass a velocity of zero to fulfil the circular movement a pulse in deviation can be detected. This effect can be reduced by implementing the friction compensation mentioned earlier as seen in the middle of Figure 11 (a). In this case the compensation works efficiently only for some areas of the circle. While in other areas, a negative pulse in deviation is detected due to overcompensation.

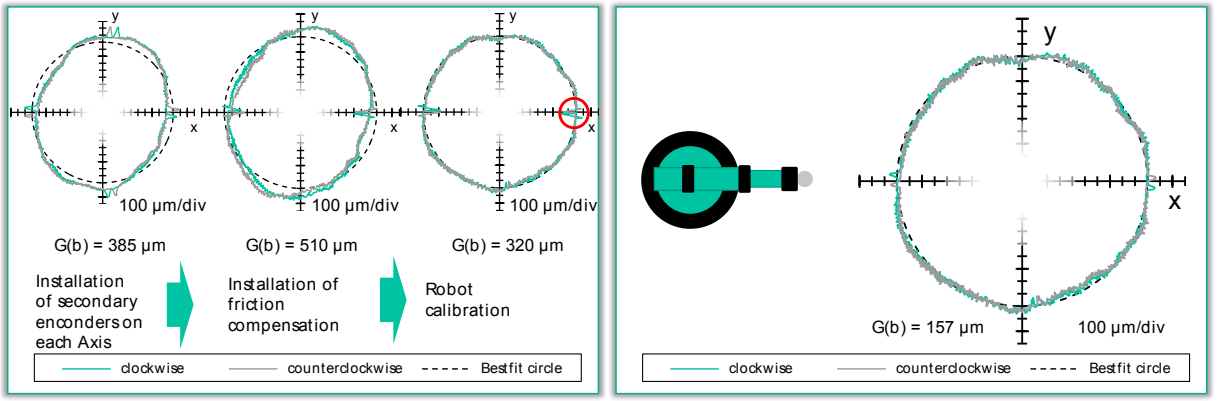

Figure 11. Development processes and improvements (a) and final result of circular test

The next step to achieve good results of circular test is the calibration of the robot including the secondary measurement system. The result of the circular test after this calibration is shown on the right of Figure 11 (a). Compared to the results without calibration, the bi-directional circular deviation is strongly reduced. Thus, the overcompensation of friction is the main cause for the remaining error as highlighted in red. The cause of this is direction reversal of axes two and three during the circular movement. By adjusting friction compensation of axis two and three again, the bi-directional circular deviation can be reduced to 157 µm. The final result is shown in Figure 11 (b).

The overall results of the ballbar tests show significant improvements for the path accuracy and repeatability. It should be noted, that secondary encoders alone do not reach the high goals for machining robots. However, in combination with advanced control strategies the iterative improvements can be seen in this paper, resulting in halved bi-directional repeatability errors. Additionally the shape of the circular tests improves significantly, which is not described by the numbers.

8. Conclusion

The present paper shows the general challenges for machining of larges CFRP parts with industrial robots for aerospace production. The workpiece size forces flexible solutions like mobile platforms to extend the robots workspace. Besides, the robot accuracy and especially the robot stiffness need improvement. One way to improve both effective stiffness and repeatability for machining operations is demonstrated with help of the implementation of secondary encoder systems and specially adapted control, calibration and compensation strategies.

The test results show clearly pros and cons of different approaches and usage of secondary encoders in combination with advanced compensation strategies. As a final result the repeatability and shape of circular movement of the industrial robot has been improved significantly by doubling the precision.

By using a standard CNC control the algorithms can easily be used in other applications or as a general product for robot manufactures in the future. The implementation of the scale tapes during construction of the robot is easy to handle and will be present in future products of *FANUC* and most probably other robot manufacturers.

It can be concluded from these results that introducing secondary encoders in industrial robots offer great potential of increasing machining accuracy with industrial robots. In combination with mobile platforms and advanced referencing technologies these systems yield promising machining concepts for machining in the aerospace factory of the future.

Acknowledgements

The present work is conducted with support of the Lower Saxony Ministry of Economics and the N-Bank following the project ProsihP II (ZW 3-80140004) led by Christian Böhlmann. The authors are grateful for the images and valuable expert information provided especially by project partners and suppliers and every member of the project team Integrated Production Systems, as well as the head of department Dr. Dirk Niermann at Fraunhofer IFAM Stade.

References

[1] Airbus S.A.S., Global Market Forecast 2016-2035: Flying by Numbers, 2016.
[2] Airbus S.A.S., Orders & deliveries | Airbus, a leading aircraft manufacturer, 2016.
[3] Boeing, Orders & Deliveries: Through May 2017, available at http://www.boeing.com/commercial/#/orders-deliveries.
[4] Abele, Polley, Ehm, Troue, Werkstatttechnik Online (2013) 706–711.
[5] M. Weigold, Kompensation der Werkzeugabdrängung bei der spanenden Bearbeitung mit Industrierobotern. Dissertation, Shaker, Aachen, Darmstadt, 2008.
[6] S. Kothe, S.P.v. Stürmer, H.C. Schmidt, C. Boehlmann, J. Wollnack, W. Hintze, Accuracy Analysis and Error Source Identification for Optimization of Robot Based Machining Systems for Aerospace Production, SAE International400 Commonwealth Drive, Warrendale, PA, United States, 2016.
[7] C. Möller, H.C. Schmidt, N.H. Shah, J. Wollnack, Enhanced Absolute Accuracy of an Industrial Milling Robot Using Stereo Camera System, Procedia Technology (2016) 389–398.
[8] H. Susemihl, C. Moeller, S. Kothe, H.C. Schmidt, N. Shah, C. Brillinger, J. Wollnack, W. Hintze, High Accuracy Mobile Robotic System for Machining of Large Aircraft Components, SAE Int. J. Aerosp. 9 (2) (2016).
[9] L. Uriarte, M. Zatarain, D. Axinte, J. Yagüe-Fabra, S. Ihlenfeldt, J. Eguia, A. Olarra, Machine tools for large parts, CIRP Annals - Manufacturing Technology 62 (2) (2013) 731–750.
[10] O. Rösch, Steigerung der Arbeitsgenauigkeit bei der Fräsbearbeitung metallischer Werkstoffe mit Industrierobotern, Utz, München, 2015.
[11] A. Ehm, Einsatz von Industrierobotern für die Bohrbearbeitung an automobilen Strukturbauteilen unter Berücksichtigung des thermischen Verlagerungsverhaltens und der Prozessinteraktion. Dissertation, 2015.
[12] G. Adams, T. Gray, D. Orf, Mobile Automated Robotic Drilling, Inspection, and Fastening (2013).
[13] FANUC, Accurate robots for high-precision applications: FANUC Secondary Encoders, available at http://www.fanuc.eu/~/media/files/pdf/products/robots/accessories/flyer secondary encoder.pdf-e0IQzrXeQ (accessed on June 30, 2017).
[14] J. Wollnack, Robotik: Analyse, Modellierung und Identifikation, available at https://www.tuhh.de/ft2/wo/Scripts/Robotik/KalKinematikModell.pdf (accessed on July 6, 2017).
[15] Amo GmbH, Product overview: Incremental & Absolute LENGTH- AND ANGLE MEASURING SYSTEMS based on the AMOSIN® – Inductive Measuring Principle, Peter am Hart, Österreich, 2017.
[16] D. Schröder, Regelung von Antriebssystemen, 3rd ed., Springer, Berlin [u.a.], 2009.
[17] M. Kurze, Modellbasierte Regelung von Robotern mit elastischen Gelenken ohne abtriebsseitige Sensorik. Dissertation, München, 2008.
[18] N. Hermann, Industrieroboter als Bearbeitungsmaschinen, Deutschland, 2014.
[19] HNI-Verlagsschriftenreihe (Ed.), Aktive Schwingungsdämpfung für Be- und Verarbeitungsmaschinen, Paderborn, 2007.
[20] K. Schröer, Identifikation von Kalibrationsparametern kinematischer Ketten, Hanser, München [etc.], 1993.
[21] H. Wittel, D. Muhs, D. Jannasch, J. Voßiek, Roloff/Matek Maschinenelemente: Normung, Berechnung, Gestaltung, 22nd ed., Springer Vieweg, Wiesbaden, 2015.
[22] International Standard, ISO 9283: Manipulating industrial robots - Performence criteria and related test methods.
[23] C. Borrmann, Adaptive Montageprozesse für CFK-Großstrukturen mittels Offline-Programmierung von Industrierobotern, 1st ed., Technische Universität Hamburg-Harburg, Institut für Produktionsmanagement und -technik, Hamburg, 2016.
[24] Hexagon Metrology, Leica absolute Tracker AT960: Product Brochure, 2015.
[25] Verein Deutscher Ingenieure / Deutsche Gesellschaft für Qualität, VDI/DGQ 3441: Statische Prüfung der Arbeits- und Positionsgenauigkeit von Werkzeugmaschinen - Grundlagen, Beuth Verlag GmbH, 2014.
[26] International Standard, ISO 230-4: Test code for machine tools - Part4: Circular tests for numerically controlled machine tools 25.040.30, 2005.